View metadata, citation and similar papers at core.ac.uk
brought to you by CORE
provided by NASA Technical Reports Server

THE ASTRONOMICAL JOURNAL VOLUME 110, NUMBER 1 JULY 1995

# SPECTRAL IRRADIANCE CALIBRATION IN THE INFRARED. IV. 1.2–35 μm SPECTRA OF SIX STANDARD STARS

MARTIN COHEN

Jamieson Science and Engineering, Inc., Suite 204, 5321 Scotts Valley Drive, Scotts Valley, California 95066 and Radio Astronomy Laboratory, 601 Campbell Hall, University of California, Berkeley 94720
Electronic mail: cohen@bkyast.berkeley.edu

NASA-CR-205317

FRED C. WITTEBORN

NASA–Ames Research Center, Mailstop 245-6, Moffett Field, California 94035-1000
Electronic mail: witteborn@ssal.arc.nasa.gov

RUSSELL G. WALKER

Jamieson Science and Engineering, Inc., Suite 204, 5321 Scotts Valley Drive, Scotts Valley, California 95066
Electronic mail: jse@netcom.com

JESSE D. BREGMAN, AND DIANE H. WOODEN

NASA–Ames Research Center, Mailstop 245-6, Moffett Field, California 94035-1000
Electronic mail: bregman@ssal.arc.nasa.gov, wooden@ssal.arc.nasa.gov

*Received 1994 December 19; revised 1995 April 3*

## ABSTRACT

We present five new absolutely calibrated continuous stellar spectra from 1.2 to 35 μm, constructed as far as possible from actual observed spectral fragments taken from the ground, the Kuiper Airborne Observatory (KAO), and the *IRAS* Low Resolution Spectrometer (LRS). These stars—β Peg, α Boo, β And, β Gem, and α Hya—augment our already created complete absolutely calibrated spectrum for α Tau. All these spectra have a common calibration pedigree. The wavelength coverage is ideal for calibration of many existing and proposed ground-based, airborne, and satellite sensors. © *1995 American Astronomical Society.*

## 1. INTRODUCTION

In a previous paper of this series we have described a consistent effort to provide absolutely calibrated broad- and narrow-band infrared photometry based upon a carefully selected, infrared-customized pair of stellar models for Vega and Sirius, created by Kurucz, and absolutely calibrated by Cohen *et al.* (1992a: hereafter referred to as Paper I). These hot stellar models have been employed as reference spectra to calibrate cool stars by the methods detailed by Cohen *et al.* (1992, hereafter referred to as Paper II), and applied to the K5III star, α Tau. This approach yields a valuable infrared-bright secondary stellar standard with a calibration pedigree directly traceable to our primary radiometric standard, namely, α CMa. This cool giant spectrum is totally unlike any blackbody in its energy distribution, and is dominated by the fundamental absorption and overtones of CO and SiO. These molecular bands are common among cool giants and supergiants (Cohen *et al.* 1992b; hereafter referred to as Paper III). By following identical procedures to those described in Paper II, we have assembled spectra for five other popular infrared "calibrators," namely β Peg, α Boo, β And, β Gem, and α Hya. In this paper we (1) graphically illustrate the techniques involved in our process of spectral assembly; (2) present all five newly built "composite" spectra, and discuss their calibration pedigrees; and (3) from them derive magnitudes in several commonly used infrared passbands. We also discuss our adopted method for extrapolation of stellar spectra to 35 μm in the absence of an observed spectral fragment, or given only a noisy spectrum, and vindicate the procedure using long-wavelength KAO data by Glaccum (1990).

## 2. THE NEW COMPOSITE SPECTRA

Our methodology for creating a complete and continuous composite spectrum from 1.2–35 μm is precisely described in Paper II. By exactly following the procedures laid down there we have been able to construct several more composites for β Peg (M2.5II–III, and the latest type we have treated), α Boo (K1III), β And (M0III), β Gem (K0III), and α Hya (K3II–III), in chronological order of actual construction. In some cases, earlier composites have been replaced by subsequent and better products, as we have acquired new and higher signal-to-noise spectral fragments either from the KAO (~5–9 μm) or from the ground (~7.5–13 μm). Cohen & Davies (1995, Paper V in this series) separately assess the calibration pedigree of the UKIRT CGS3 spectrometer that has provided most of our 10 μm spectra. Table 1 will serve as a guide to the currently available and most reliable composites and models for the eight stars within our calibration context.

We emphasize the following key points concerning spectrum assembly.

(i) We define flux density calibrations only for filters with known transmission profiles scanned at their cold operating

 0004-6256/95/110(1)/275/15/$0.90 © 1995 Am. Astron. Soc. 

TABLE 1. Model and composite spectra currently available.

| Star | Spectral type | Date of assembly |
|---|---|---|
| $\alpha$ Lyr | A0 V | July 23, 1991 |
| $\alpha$ CMa | A1 V | July 29, 1991 |
| $\alpha$ Tau | K5 III | March 5, 1992 |
| $\beta$ Peg | M2.5 II-III | March 10, 1992 |
| $\alpha$ Boo | K1 III | April 28, 1993 |
| $\beta$ And | M0 III | October 15, 1993 |
| $\beta$ Gem | K0 III | September 12, 1994 |
| $\alpha$ Hya | K3 II-III | December 12, 1994 |

points, and we incorporate the effects of terrestrial site-specific transmission through the atmosphere, and of detector quantum efficiency.

(ii) We use photometry from the literature only if errors and magnitudes of standard stars are given so we can calculate the relevant "zero point offsets" (i.e., we define Vega to have zero magnitude at all infrared wavelengths; others may not do so, thereby creating an "offset" from zero in their system relative to our own).

(iii) All fragments are calibrated by multiplying the observed ratios of matched airmass spectra of a cool star and a reference star (Sirius or Vega) by the calibrated Kurucz hot star model, after convolution with a Gaussian that represents the combined effects of the instrumental profile with the actual spectral observations (cf. Appendix B and Fig. 14 of Wooden *et al.* 1993).

(iv) We stress independent photometric calibration of every possible spectral fragment by all possible filters whose passbands are entirely contained within the observed fragment.

(v) In the regions of overlap of two independent spectral fragments, both are combined using inverse variance weighting.

(vi) No fragment is ever changed in shape (except where it overlaps another fragment), only shifted in the absolute level.

(vii) The order of operations (Paper II) is logical but not important to the end product: we normalize the 1–5 $\mu$m fragment to near-infrared photometry; we separately but identically treat the 7.5–13 $\mu$m fragment using narrow band photometry in the 10 $\mu$m region; we splice the LRS 7.7–22.7 $\mu$m spectrum to the higher resolution CGS3 10 $\mu$m fragment (degrading the resolution of the CGS3 spectrum to match that of the LRS before splicing); we doubly splice the KAO 5–9 $\mu$m fragment to both the radiometrically calibrated 1–5 and 8–23 $\mu$m pieces; we then splice other long wave fragments to the long-wavelength observations.

We illustrate the following three primary procedures explicitly. (Note that in our graphics we make use of $\lambda^4 F_\lambda$ vs $\lambda$ plots; these mitigate the intrinsically very steep falloff of stellar continua and enable us to display spectral fragments linearly for clarity.)

(viii) Normalization of a fragment with respect to photometry—Fig. 1 shows the Strecker *et al.* (1979, hereafter referred to as SEW) $\alpha$ Tau fragment placed relative to the

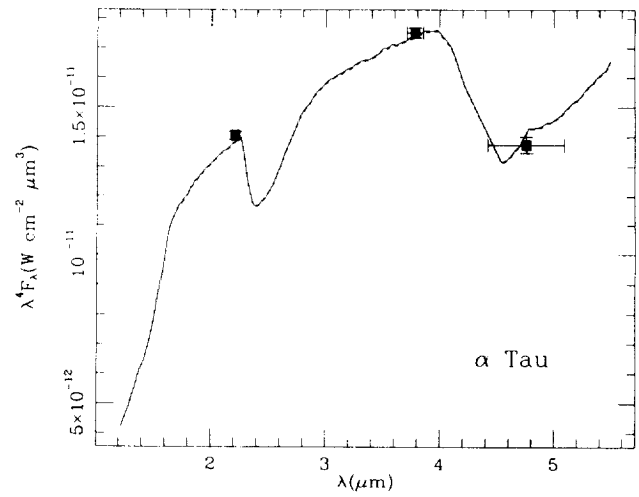


FIG. 1. Strecker *et al.* (1979) 1.2–5.5 $\mu$m KAO fragment for $\alpha$ Tau located with respect to photometry (Kn, Ln, M). The $\pm$HWHMs of the relevant passbands are plotted. The short dashed line (barely distinguishable from the solid) is the SEW fragment; the solid line is the result of scaling it by 1.003 to fit this photometry.

Selby *et al.* (1988) "Kn" and "Ln" points, and the UKIRT (Deacon 1991) "M" point. The multiplier for the fragment is the inverse variance weighted result of simultaneously matching (in a least-squares sense) the three in-band flux ratios (KnLnM) defined from the $\alpha$ Tau fragment ratioed to the $\alpha$ Lyr calibrated model (Paper I). The short-dashed line represents the SEW fragment (after correction to the context of our 1991 Kurucz Vega model and for the influence of the potential nonlinearity in wavelength in the SEW longest filter wheel: cf. Figs. 5 and 6 of Paper II); solid line, barely perceptibly different from the solid (the scale factor applied was 1.003), is our rescaled version of the SEW spectrum.

(ix) A single-sided splice—in Fig. 2, the UKIRT CGS3

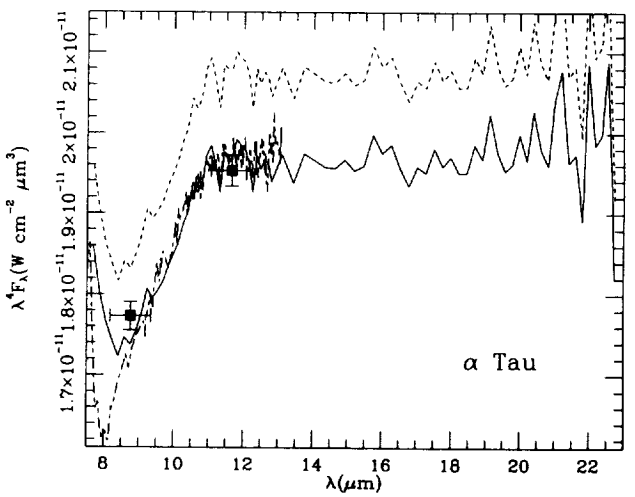


FIG. 2. A single-sided splice of the *IRAS* LRS spectrum of $\alpha$ Tau with the higher resolution UKIRT CGS3 spectrum (long-dashed–short-dashed line), which was previously "locked" to photometry from UKIRT ([8.7], [11.7]). The short-dashed line is the original LRS fragment; the solid line is the LRS scaled by 0.95. Note the close accord of the shapes of the rescaled LRS spectrum and the ground-based CGS3 spectrum. Deacon's (1991) photometry is included (along with the $\pm$HWHMs of the passbands).

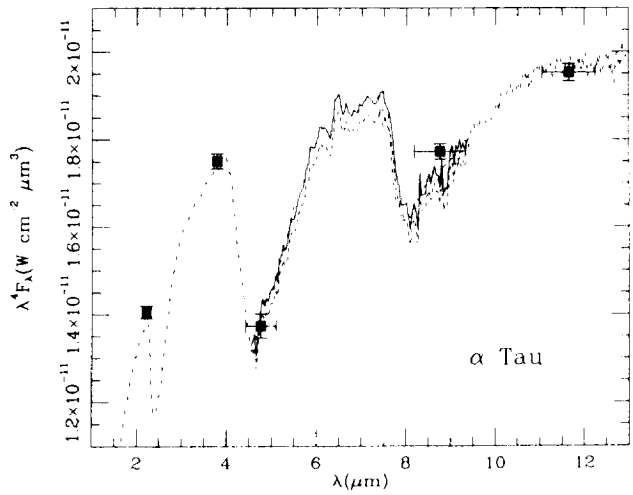


FIG. 3. Double-sided splice of the KAO fragment of $\alpha$ Tau to the radiometrically calibrated 1.2–5.5 and 7.5–22.7 $\mu$m pieces. The KAO fragment fits between the other two; the unscaled KAO portion is the short-dashed 5–9 $\mu$m piece; the solid line is the same fragment scaled by 1.022. All the photometry used to assemble the complete $\alpha$ Tau spectrum appears here, together with the passband ±HWHMs.

fragment is first "locked" to the [8.7] and [11.7] magnitudes shown in this figure (rescaling by 1.039) then $\alpha$ Tau's original LRS spectrum (short dashed line) is spliced to the CGS3 spectrum giving the solid line (the multiplier was approximately 0.95). Note that the higher resolution CGS3 spectrum was first degraded to match the LRS in resolution, before splicing. This figure details the region of overlap between these two fragments.

(x) A double-sided splice—in Fig. 3, $\alpha$ Tau's KAO spectrum is inserted between the radiometrically calibrated near- and mid-infrared spectra, simultaneously minimizing differences in the pair of jointly overlapping wavelength regions in a least-squares sense. The multiplier here is 1.022, moving the KAO fragment from the short dashed line to the solid line.

Figure 4 presents all six cool stellar composites in the form of absolute log($\lambda^4F_\lambda$) plots against log($\lambda$). In each spectrum, the $\pm1\sigma$ error range is indicated. Note that, for $\alpha$ Tau, the entire 1.2–35 $\mu$m range was spanned by observations through the fortuitous efforts of Glaccum (1990) who obtained 16–35 $\mu$m KAO spectra, which usefully extended the typical observation limit of 22.7 $\mu$m of the LRS instrument, or ~24 $\mu$m from UKIRT CGS3 long-wavelength spectroscopy from Mauna Kea. No other star among our composites has such a long-wavelength KAO fragment although occasionally we can extend the LRS range slightly using CGS3 data from 16 to 24 $\mu$m. Therefore, we need a method of extrapolation beyond the 20 $\mu$m domain.

After careful examination of all our spectral fragments, and of a number of model atmospheres for $\alpha$ Tau built by D. Carbon (1994), we decided to adopt the Engelke (1992) function as an extrapolator for the stellar continuum. The long dashed curves in Fig. 4 represent the relevant Engelke functions for the five composites. This analytic approximation to real stellar continua was derived assuming that the dominant source of infrared continuum opacity in these cool giant stars is $H^-$ free–free. The intensive CRAY computations of $\alpha$ Tau's atmosphere by Carbon (1994) demonstrate that the Engelke function is a reasonably good approximation to the theoretical continuum at all wavelengths between 2 and 35 $\mu$m (it lies within ~±5% of the full-blown calculation). It is pertinent to ask whether we have substantive evidence that real stars behave in the way suggested by any of these models or approximations. Glaccum (1990) has observed the spectra of two normal stars (not known variables and without dust shells) between 16 and 35 $\mu$m from the KAO. Both the Engelke function and the CRAY models represent quite well the *observed* continuum in $\alpha$ Tau (Fig. 14 of Paper II; Fig. 5 of Paper III) and in the M3.5III $\gamma$ Cru (Fig. 5). The importance of these KAO measurements is that their calibrational pedigree is entirely independent of any aspect of stars and their behavior. It is founded on observations and models for Uranus and Mars (cf. Moseley *et al.* 1989). Paper II illustrates the observed featureless and Rayleigh–Jeans character (flat in $\lambda^4F_\lambda$ space) of the $\alpha$ Tau spectrum as far as 35 $\mu$m. Figure 5 demonstrates the same behavior for $\gamma$ Cru, comparing the observed LRS and Glaccum KAO spectra with the shape of the Engelke function for this star. These long-wavelength KAO spectra materially strengthen our belief in the validity of these flat extrapolations of stellar spectra in the limited domain over which we use them (10–35 $\mu$m at most). By splicing Engelke functions to the actual composite observations longward of the SiO fundamental (typically, between about 12 and 22 $\mu$m), we can establish the flux density level of this spectral approximation, and hence estimate the stellar angular diameter.

We have also chosen to substitute this best-fitting Engelke function for noisy LRS and/or 20 $\mu$m CGS3 data when appropriate. Figure 6 exemplifies this substitution process for $\beta$ And where both LRS and long-wave CGS3 fragments are available, but both are noisy in this amplified portrayal in a $\lambda^4F_\lambda$ plot. There is no meaningful overlap between the two fragments; i.e., the 20 $\mu$m CGS3 fragment is unconstrained in the absolute level. The Engelke function seems to represent the *shape* of these two fragments very well. Even though noisy, these observed spectra are flat overall, or we would not be justified in using this simplistic substitution. (The same situation arises for $\beta$ Gem.)

The essential parameters for the Engelke function, namely effective temperature and angular diameter, are initially fixed by reference to the work of Blackwell *et al.* (1991). $T_{\rm eff}$ is never altered; only the angular diameter is (slightly) rescaled when the Engelke function is spliced to our observed spectra. We do, however, assign a conservative uncertainty of a few percent to any usage of this approximation, driven largely by the uncertainties in both $T_{\rm eff}$ and angular diameter estimated by Blackwell *et al.* (1991), but also taking note of the change in infrared slope of the Engelke function engendered by the uncertainty in stellar temperature. We note that Blackwell & Lynas-Gray (1994) have recently recalibrated their narrow band near-infrared photometry of bright stars to which they apply the "Infrared Flux Method." They have redetermined both $T_{\rm eff}$ and angular diameter for many stars, including $\beta$ Gem, where their new determination (8.03 milliarcsec [mas])

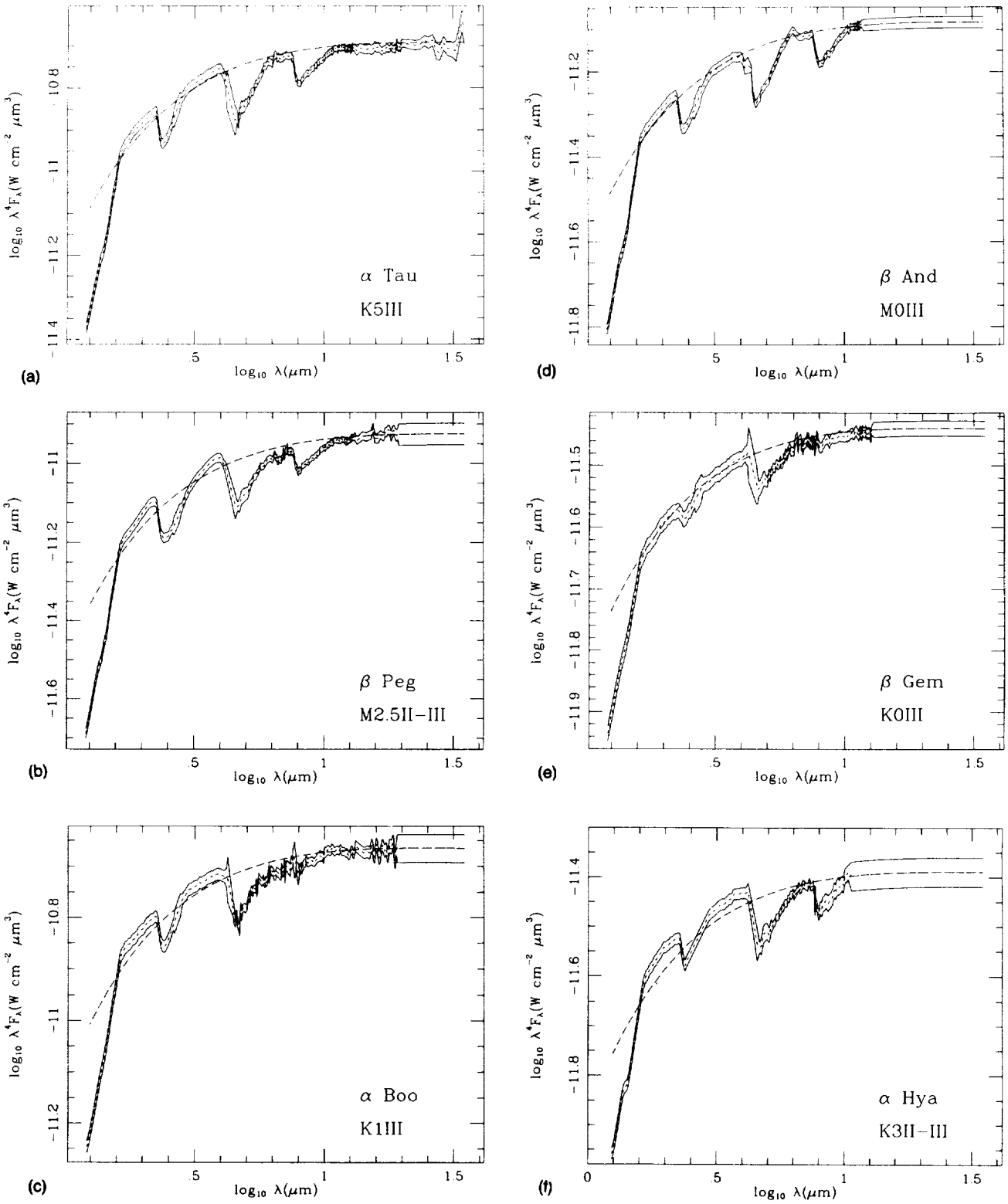


FIG. 4. All six cool stellar composites in the form of logarithmic plots of absolute $\lambda^4 F_\lambda$ against $\lambda$. In each spectrum, the $\pm 1\sigma$ error bars are indicated by the pair of solid lines, with the mean spectrum represented by the short-dashed line. The long-dashed line is the best-fitting Engelke approximation. (a) $\alpha$ Tau; (b) $\beta$ Peg; (c) $\alpha$ Boo; (d) $\beta$ And; (e) $\beta$ Gem; and (f) $\alpha$ Hya.

agrees very well with our own, via normalization of an Engelke function (8.07 mas).

These functions play a useful role in all five new stellar composites, to varying degrees, depending essentially on the quality of the longest-wavelength LRS data. Table 2 summarizes details of these substitutions in our composites (or, for the completely observed $\alpha$ Tau, the value of the best-fitting Engelke function for the overall spectrum, even though one is not used in the actual spectrum assembly). Of those molecules that one would incorporate into a full model atmosphere calculation, only $CO_2$ might be relevant and has any strong absorption bands between about 12 $\mu$m (by which

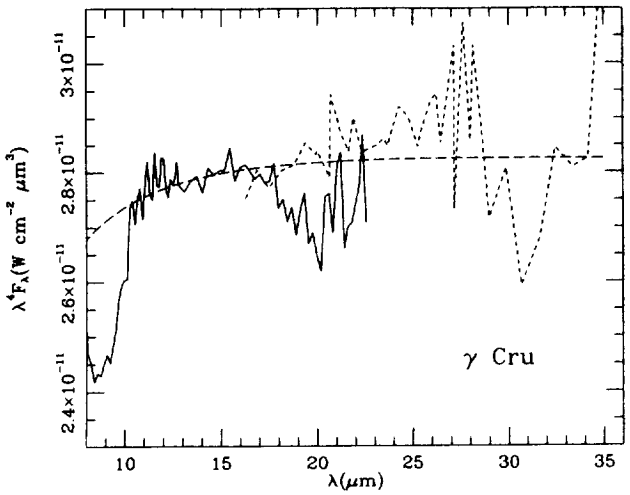


FIG. 5. The two independently calibrated long-wavelength fragments of the mid-M giant, $\gamma$ Cru. The shorter spectrum is from the *IRAS* LRS; the longer from Glaccum's (1990) work. In spite of the noise (note that a $\lambda^4 F_\lambda$ plot acts as an amplifier of any inherent noise), one definitely sees indications in these axes of a sustained "flat" spectrum out to 35 $\mu$m, as for $\alpha$ Tau; i.e., a Rayleigh–Jeans character.

wavelength the SiO fundamental has essentially disappeared at our relatively low resolution) and 35 $\mu$m. However, its expected abundance in these cool giants is orders of magnitude below those of CO and SiO. It is, therefore, very plausible that a pure continuum extrapolation of these composites is justified at long wavelengths. While the Engelke function matches the continuum regions of our warmest star ($\beta$ Gem) very well and those of our coolest ($\beta$ Peg) most poorly (Fig. 4), we see no overall systematics with respect to effective temperature. These functions seem to fit all these cool giants equally though they are at best only approximations at the $3\sigma$ level, sometimes above and at other times below the observed continua. There is a tendency for the function that best fits the long wavelengths to fall significantly below the

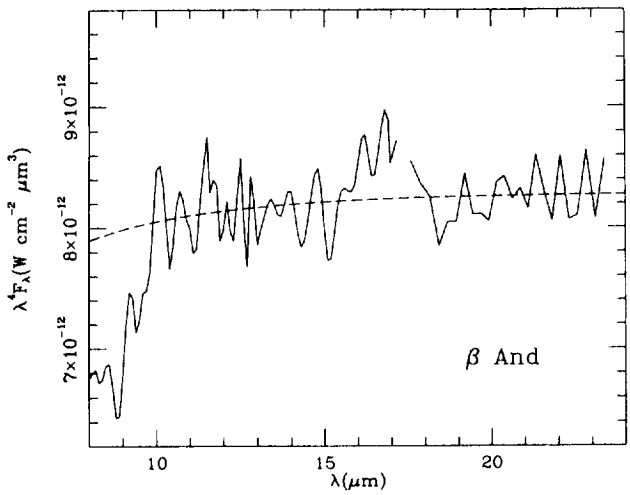


FIG. 6. The two observed, but noisy, long-wavelength fragments of $\beta$ And and the Engelke function used as their substitute. The portion from 8 to about 17 $\mu$m is the LRS which was truncated due to high noise beyond 17 $\mu$m; that longward of about 17.5 $\mu$m represents the useful part of a UKIRT CGS3 spectrum in the 16–24 $\mu$m range.

TABLE 2. Engelke functions used in, or relevant to, composite spectra.

| Star | Effective Temperature (K) | Angular diameter milliarcsec |
|---|---|---|
| $\alpha$ Tau | 3898 | 21.32 |
| $\beta$ Peg | 3600 | 16.98 |
| $\alpha$ Boo | 4362 | 20.80 |
| $\beta$ And | 3839 | 13.71 |
| $\beta$ Gem | 4866 | 8.07 |
| $\alpha$ Hya | 4141 | 9.27 |

near-infrared continua, perhaps reflecting the fact that the approximation is strictly valid only in the context of solar-type stars. In these cooler objects, one might well expect $H^-$ free–free opacity to lose its dominating influence to molecular opacity.

## 3. NEW SPECTRAL FRAGMENTS

All the new spectral fragments incorporated into this paper were secured with one or more of the following instruments: the NASA–Ames "SIRAS" (Short-Wavelength Infrared Array Spectrometer; Wooden 1989), "FOGS" (Faint Object Grating Spectrometer; Witteborn & Bregman 1984), or "HIFOGS" (High-efficiency Infrared Faint Object Grating Spectrometer; Witteborn *et al.* 1995) on the KAO or with the NASA 1.5 m Mount Lemmon telescope; or the CGS3 spectrometer on the 3.8 m UKIRT. The Ames spectrometers are doubly sampled by using two different grating settings spaced a few detectors apart to achieve Nyquist sampling and to provide coverage of occasional dead detectors. CGS3 is either doubly or triply sampled, likewise to achieve the full theoretical resolution. For the CGS3 fragments (cf. Cohen & Davies 1995) we have always stressed close matching of airmasses between the target (cool) star and the hot reference object (Sirius or Vega). From the KAO we cannot always exert such control over stellar airmasses at the time of observation due to the relative brevity and constraints of the actual observing time at altitude. Therefore, we remove the residual effects of the terrestrial atmosphere (particularly important from 5–8 $\mu$m) *post facto* from the spectra, through use of precomputed standard atmospheric transmission curves relevant to different amounts of precipitable water vapor (currently between 6 and 12 $\mu$m). Actual water vapor is measured on each flight with a radiometer. These transmissions are calculated using Lord's (1992) ATRAN tool.

One of the goals of our overall effort has been to provide a composite spectrum for every cool giant spectral type. Therefore, we have for some time been trying to secure observations of a K3 III. SEW provide coverage in the 1.2–5.5 $\mu$m range for only $\gamma^1$ And, of type K3-IIb, but we have never been able to acquire adequate 5–9 $\mu$m data of this star. However, $\alpha$ Hya (K3 II–III) was frequently observed during KAO expeditions to New Zealand to monitor SN 1987A, and Sirius was usually observed on the same flights. Consequently, we have elected to construct a composite for $\alpha$ Hya whose NIR fragment is actually that of $\gamma^1$ And, very closely matched in type. In defense of this procedure we note that the bias associated with the normalization of $\gamma^1$ And's NIR

spectrum to the actual photometry of $\alpha$ Hya is only 0.50% (Table 8), implying that these five photometric points for $\alpha$ Hya accurately match the shape defined by this miniature template.

## 4. PHOTOMETRY USED

Supporting photometry for these spectral assemblies comes, as in Paper II, almost entirely from Deacon's (1991) tabulations for the UKIRT M, 8.7 and 11.7 $\mu$m passbands, and from Selby *et al.* (1988) for the extremely valuable narrow band Kn and Ln measurements. All photometry that we use to construct a composite appears in the individual informational header (see Tables 4–8). A final check is later performed on each composite to see how well it fits *all* available characterized filter photometry, as opposed to just the five measurements already employed. Typically this involves 12–20 measurements between 1.6 and 25 $\mu$m. The normalization factors for each composite lie within $\pm$0.004 of unity, thereby validating the overall construct and ruling out conspicuous infrared photometric variability in any of these stars within the period covered by the available characterized photometry. After construction we also integrate the composite over all available combinations of filter and detector and atmosphere that we have archived, thereby providing a refined set of actual magnitudes (as opposed to those estimated from the literature). Because of their widespread usefulness, we have included a subset of these magnitudes in Table 3. These refer strictly to the passbands characterized in Paper I but will also represent the magnitudes (within 0.01–0.02 mag) at typical lower elevation sites. We can, of course, create "customized" photometry for *any* triad of filter, detector, and atmosphere given the actual system (or separate passband) profile(s) measured cold.

It is important to distinguish between the photometry that is instrumental in creating the complete spectrum, and that used *post facto* to validate the composite spectrum. The former includes two of the narrow bands created by Selby *et al.* (1988), namely Kn and Ln, and three UKIRT bolometer points for M, [8.7], and [11.7]. Due to the anchoring role played by these filters, we discuss the out-of-band rejection of these passbands, and give some history of the actual magnitudes used for most of our stars.

It is the fundamental tenet of our calibration philosophy that photometry produces the most accurate radiometric levels while one tasks a spectrometer with providing accurate spectral shapes. This belief stems from the all too frequent usage with IR spectrometers of small apertures that cannot capture all the light (cf. Cohen & Davies 1995), and from the strong likelihood that different seeing conditions will prevail while target and reference stars are being separately observed. In Paper II we, therefore, developed a procedure of using independently obtained and calibrated photometry to normalize IR spectral shapes to their correct radiometric levels. *This tenet and our broad-wavelength, multifragment method distinguish our approach from all other efforts in this field.*

Our procedure is first to lock the SEW (1.2–5.5 $\mu$m) KAO fragment to Selby *et al.*'s (1988) narrow band photometry in the Kn and Ln bands, and to UKIRT M photometry. These two Selby filters were very carefully selected to sample the cleanest parts of the terrestrial atmospheric transmission curve in the general vicinities of the conventional broadband K and L′ passbands. They are only 0.05 and 0.14 $\mu$m in FWHM, respectively, and we have vindicated the contention that these are robust bandpasses by calculating the isophotal wavelengths and transmission-weighted monochromatic flux densities for these when used at Mauna Kea and at a lower elevation site (Tables 1 and 2 of Paper I). There are no differences with site (using annual average transmission curves for each site's observing season) in either isophotal wavelength (Paper I) or $F_\lambda$. The choice of the filters was originally motivated by equally rigorous work on the absolute IR calibration of Vega (Mountain *et al.* 1985; Leggett *et al.* 1986; Blackwell *et al.* 1991).

Both Kn and Ln are defined by tandem filters, one narrow band, and the other conventional (the latter are the UKIRT standard K and L′ bands), each component separately specified to have out-of-band rejections of $10^{-4}$ or better from the UV to at least 10 $\mu$m (Leggett 1994; Mountain 1994; Petford 1994) The separate transmission curves of the filter elements of these tandem combinations were measured in the laboratory at 78 K by Selby (documentation is most complete for the laboratory sessions of July 1, 1981, July 12, and September 13, 1982), using a specially designed monochromator and an absolutely calibrated furnace (typically run at 1254 K). He determined there were no out-of-band leaks greater than $10^{-4}$ of the peak transmission in any of the standard UKIRT filter set (JHKLL′M), which includes the two (K,L′) used as broadband blocking filters for Kn and Ln. The narrow band tandem combinations were regularly measured in their usual cryostat before and after observing sessions at Tenerife by Selby (Petford 1994), with the same equipment and yielded similar results. Best documented are actual mea-

TABLE 3. (a) Refined near-infrared magnitudes derived *post facto* from our model and composite spectra. Passbands are as declared in Paper I. (b) Refined mid-infrared magnitudes derived *post facto* from our model and composite spectra. Passbands are as declared in Paper I.

(a)

| Star | Jn | Kn | Ln | J | H | K | L | L′ | M |
|---|---|---|---|---|---|---|---|---|---|
| $\alpha$ Lyr | 0.00 | 0.00 | 0.00 | 0.00 | 0.00 | 0.00 | 0.00 | 0.00 | 0.00 |
| $\alpha$ CMa | -1.39 | -1.37 | -1.36 | -1.39 | -1.40 | -1.37 | -1.36 | -1.36 | -1.36 |
| $\beta$ Gem | -0.55 | -1.14 | -1.23 | -0.40 | -1.04 | -1.12 | -1.20 | -1.22 | -1.09 |
| $\alpha$ Boo | -2.27 | -3.07 | -3.17 | -2.14 | -2.96 | -3.04 | -3.15 | -3.15 | -2.93 |
| $\alpha$ Hya | -0.44 | -1.26 | -1.38 | -0.30 | -1.11 | -1.22 | -1.35 | -1.36 | -1.12 |
| $\alpha$ Tau | -1.97 | -2.93 | -3.06 | -1.84 | -2.74 | -2.90 | -3.04 | -3.05 | -2.77 |
| $\beta$ And | -0.89 | -1.93 | -2.05 | -0.78 | -1.73 | -1.89 | -2.02 | -2.02 | -1.78 |
| $\beta$ Peg | -1.18 | -2.33 | -2.49 | -1.09 | -2.09 | -2.29 | -2.45 | -2.47 | -2.20 |

(b)

| Star | 8.7 | N | 11.7 | Q | IRAS12 | IRAS25 |
|---|---|---|---|---|---|---|
| $\alpha$ Lyr | 0.00 | 0.00 | 0.00 | 0.00 | 0.00 | – |
| $\alpha$ CMa | -1.35 | -1.35 | -1.35 | -1.34 | -1.35 | -1.34 |
| $\beta$ Gem | -1.21 | -1.22 | -1.22 | -1.23 | -1.22 | -1.22 |
| $\alpha$ Boo | -3.12 | -3.14 | -3.16 | -3.16 | -3.15 | -3.16 |
| $\alpha$ Hya | -1.25 | -1.31 | -1.35 | -1.35 | -1.35 | -1.35 |
| $\alpha$ Tau | -2.95 | -3.02 | -3.07 | -3.08 | -3.08 | -3.10 |
| $\beta$ And | -1.96 | -2.05 | -2.11 | -2.12 | -2.11 | -2.12 |
| $\beta$ Peg | -2.37 | -2.44 | -2.49 | -2.51 | -2.48 | -2.51 |

surements made on November 17, 1980 with the furnace and monochromator. Blocking of Kn and Ln were found to be superior to $10^{-5}$ and likely to be no poorer than $10^{-6}$. Such values are also cited by both Leggett (1994) and Mountain (1994), whose Ph.D. dissertations depended on these passbands. For example, Leggett's thesis stipulates "The narrow band filters were blocked by wider filters to reduce any filter leakage. We searched for leakage on site using the furnace with combinations of warm and cold filters. The leakage of *unblocked* filters was estimated to be $\leq 0.01\%$." Hence, blocked filter leakage was much superior to this figure of 0.01%.

Realizing just how difficult and important were their attempts to calibrate Vega absolutely, Blackwell, Selby, Mountain, and Leggett in their various efforts and publications were at pains to detail all possible sources of uncertainty, down to the component level. The DC linearity of the InSb system overall was of great concern (cf. Mountain *et al.* 1985) and forms the substance of a separate and detailed document (McGregor 1977). In particular, the Ohmic properties of the Victoreen feedback resistors (the dominant source of potential concern) were established to be linear to better than 0.5%. The detectors were (and still are) run in low voltage and low-current circumstances. High voltages would occasion far more concern in terms of possible nonlinearities and the figure of $<0.5\%$ was obtained even when measuring signals far higher than those due to stars on the relevant telescope. The amplifier chains have been, and are still, regularly measured and found to harbor no nonlinearities above the 0.01% level and their gains are well calibrated (Hammersley 1994). Questions of potential saturation, and hence nonlinearities, may also arise in the context of a comparison between stars as bright as $\alpha$ Tau with Vega. The InSb system in question has a very large dynamic range. This multichannel narrow band system is still in frequent use in The Canaries on both 1.5 m and 4.5 m telescopes. No saturation effects have been detected in use on stars with the flux densities of $\alpha$ Tau even on the 4.5 m (William Herschel) telescope. Stars as faint as K=18 or fainter are routinely measured so the dynamic range in the linear regime of detector/system behavior is established to be far larger than the span between infrared-bright stars like $\alpha$ Tau and Vega. The use of the doubly blocked narrow band filters on the 1.5 m telescope employed by Blackwell and colleagues, *a fortiori* excludes any possibility of detector saturation. In addition, as detailed by Mountain *et al.* (1985), the original calibration work involved direct comparison of Vega with an absolute furnace on the telescope. The issues of dynamic range and saturation were, therefore, central to the measurements made by these authors, hence their painstaking efforts to assure that no source of potential error was overlooked.

In our spectral assembly scheme (Paper II) we next lock the CGS3 fragment (typically from 7.4–13.4 $\mu$m) to [8.7] and [11.7] photometry obtained from the UKIRT using their standard bolometer (UKT8) with characterized cold filter transmission curves. Rejection was measured in July 1982 by Beattie at the Royal Observatory Edinburgh at the request of Barlow and Cohen. A series of documented experiments was also carried out at Mauna Kea using UKIRT on July 27, 1982 and combining these internal cold filters with external warm ones in the 10 $\mu$m region. Memoranda indicate "zero" signals were detected through these combinations, with implied rejections of at least $3\times10^{-5}$, or better, out of band. Issues of linearity were again covered in McGregor's (1977) report.

The actual magnitudes of the five stars in the Kn, Ln, M, 8.7, and 11.7 $\mu$m filters (in a context in which Vega is 0.000 at all wavelengths) that we used to assemble their composite spectra are summarized in Tables 4–8 (and Paper II). The sources for photometry and assigned uncertainties are Selby *et al.* (1988) and Deacon (1991). The 8.7 and 11.7 $\mu$m pair of filters is critical to calibrating our 10 $\mu$m spectral fragments for any star. Therefore, we append here the typical details of this narrow band 10 $\mu$m photometry for one star in order to characterize the dataset that constitutes Deacon's table of photometry for "standard stars." Because we use $\alpha$ Tau to illustrate spectrum assembly we will also use its photometry to exemplify the pedigree of Deacon's tabulated magnitudes.

There are several distinct elements to this photometry, one of which is based on measurements with germanium bolometers actually made by Cohen and Barlow over a 13 yr period (August 1976–August 1989) from several telescopes: the 3.8 m UKIRT, the 1.5 m at Cerro Tololo, the 1.3 m at Kitt Peak, and the Minnesota–San Diego Mount Lemmon Observatory 1.5 m. Cohen and Barlow were able to construct a set of midinfrared magnitudes from these hundreds of standard star measurements akin to those by Thomas *et al.* (1973), Gehrz *et al.* (1974), Cohen & Barlow (1974, 1980). Of these measurements, the magnitudes relevant to our spectral calibration effort are solely those for M, [8.7], and [11.7]. For M. Deacon (1991) took the published spectrophotometry of SEW for bright standard stars and integrated these spectra through the combination of the cold system (UKIRT) passband and the Mauna Kea atmosphere. These provided M data for stars such as $\alpha$ Tau and $\beta$ Peg relative to Vega (adopted to be zero magnitude at all wavelengths shortward of 20 $\mu$m). The reproducibility of the SEW dataset was found to be no worse than 2% in absolute signal and shape (cf. SEW) so these relative magnitudes are felt to be good to about $\pm0.02$, a value defensible by comparison with the Cohen and Barlow broadband archive. Use of an airborne spectral archive to define stellar M brightness with respect to Vega (zero magnitude) leads to a much more reliable determination even for relative magnitudes than typical ground-based observations. The 5 $\mu$m "window" is notoriously variable in time from the ground but observations are considerably more reproducible from 12.5 km altitude.

The second element is the set of [8.7] magnitudes. These were most precisely systematized during 1980 and 1981 using the UKT8 bolometer on the UKIRT telescope, although values good to $\pm0.02$–0.03 were already available in the literature. Nights were clear, calm, and mostly quite transparent. During six nights (UT 1980 September 1 and 3, 1981 October 18, 19, 20, and 21) we made 92 measurements of standard stars, referring the cool giants to both Vega and Sirius to establish accurate and traceable zero points for [8.7]. Conditions were quite stable: zero points reproduced to within a few percent and resulted in sensible extinction val-

ues. Extinction in this filter varied during the overall observing runs between 0.05 and 0.60 mag/AM, but the average value for the relevant six nights was better defined, at 0.11 ±0.05 mag/AM. We concentrated on defining relative magnitudes between a cool giant and either Vega or Sirius, with minimal airmass differences between the pairs. A typical cool star had ten measurements relative to either Vega or Sirius, and we used an aperture of diameter 8 arcsec with UKT8. Below we summarize the salient measurements for $\alpha$ Tau in [8.7].

**1980, August 31**. The observed values of Δ[8.7] between $\alpha$ Tau and $\alpha$ Lyr were $-3.03\pm0.03$ with airmasses of 1.02 and 1.06, respectively, while a second set gave $-3.00\pm0.01$ with airmasses of 1.03 and 1.10, respectively (extinction at 8.7 $\mu$m was measured at 0.05±0.05 mag/AM). With Vega as 0.00 these magnitude differences translate directly into the magnitude of $\alpha$ Tau.

**1981, October 17**. The observed value of Δ[8.7] between $\alpha$ Tau and $\alpha$ CMa was $-1.61\pm0.01$, with airmasses of 1.37 and 1.26, respectively. Extinction was measured at 0.16 ±0.05 mag/AM for the October 17–19, 1981 period so from this we find $\alpha$ Tau has $[8.7]=-2.98\pm0.01$, with $\alpha$ CMa as $[8.7]=-1.35$ (Paper I). A second set of measurements between the same pair of stars on this night yielded $\Delta[8.7]=-1.68\pm0.01$ with airmasses of 1.05 and 1.64, respectively, when $[8.7]=-2.93\pm0.03$.

**1981, October 18**. The observed value of Δ[8.7] between $\alpha$ Tau and $\alpha$ CMa was $-1.63\pm0.01$, with airmasses of 1.18 and 1.25, respectively. From this we find $\alpha$ Tau has $[8.7]=-2.97\pm0.01$.

**1981, October 19**. The observed value of Δ[8.7] between $\alpha$ Tau and $\alpha$ Lyr was $-2.97\pm0.01$, with airmasses of 1.14 and 1.02, respectively. From this we find $\alpha$ Tau has $[8.7]=-2.99\pm0.02$. On the same night, Δ[8.7] between $\alpha$ Tau and $\alpha$ CMa was $-1.59\pm0.01$, with airmasses of 1.02 and 1.25, respectively; whence $[8.7]=-2.90\pm0.02$.

By inverse variance weighting we finally obtain $\alpha$ Tau's [8.7] as $-2.97\pm0.01$.

We note that recent independent determinations by Hanner (1994) at the IRTF yield $[8.7]=-2.97\pm0.02$ for $\alpha$ Tau, in a filter similar to the cold characterized UKIRT 8.7. This, too, is in the context of Vega as zero magnitude.

The third element is [11.7] data. Because a homogeneous exoatmospheric archive like *IRAS* is not subject to the vagaries of transparency or extinction changes which occur even on Mauna Kea, and due to the close proximity of central wavelengths between the *IRAS* 12 and the UKIRT 11.7 $\mu$m bands, we believe it to be far more secure to derive the precise value of [11.7] for $\alpha$ Tau directly from [12]. Deacon (1991) has presented an analysis of *IRAS* flux densities obtained for a number of IR-bright "calibrators." He placed heavy reliance on the *IRAS* Pointed Observation archive at Rutherford Laboratory, in particular on measurements with the "DPP" macros taken by Barlow and Willis, augmented by "DPS" macros (cf. Tables 3.1 and 3.2 on Young *et al.* 1985) and later by the body of the Serendipitous Survey Catalog (Kleinmann *et al.* 1986). Although Point Source Catalog (1988, hereafter referred to as PSC) data were also used these *IRAS* Pointed Observations (PO) clearly have higher significance. The issue is not one of signal to noise ratio (SNR): all these bright cool giants have large formal SNR in the PSC but their "RELUNC" values (the relative uncertainties taking into account any systematics and the time since the last internal stimulator flashes) are generally a few percent. By contrast, the PO data have less intrinsic scatter than PSC measurements and contain their own contemporaneous stimulator flashes. Indeed, Aumann *et al.* (1984) have documented the accuracy of PO at 1% in [12], rather better than the precision attainable from the ground even with large telescopes. Consequently, Deacon was able to determine that $\alpha$ Tau has a [12] of $-3.05\pm0.01$.

In his dissertation Deacon used standard IR philosophy in extrapolating monochromatic flux densities from 12 to 11.7 $\mu$m, namely to posit that $\alpha$ Tau behaves as a Planck function at its effective temperature. With hindsight (e.g., Paper II) we would now argue that a far better representation for $\alpha$ Tau is to assert that, longward of the obvious SiO fundamental absorption in K and M giants, stars are already in the domain where $F_\lambda \propto \lambda^{-4}$. This asymptotic domain is not attained by Planck functions or stellar models for stellar temperatures by 12 $\mu$m, but real stars appear to have true Rayleigh–Jeans (RJ) spectra by this wavelength. Because the wavelength difference between 11.7 and 12 $\mu$m is so tiny, the difference between a true RJ slope in this wavelength region and an actual model atmospheric spectrum (or even a Planck function) for cool giants is virtually negligible. Hence the difference in deduced [11.7] between the strictly incorrect blackbody assumption and the more accurate RJ method is only 0.004 mag in modulus. This calculation indicates that Deacon's methodology and tabulated magnitudes (for all relevant K and M giants in his Table 2.4) are meaningfully converted from [12] to [11.7], to much better than 0.01 mag.

For photometry to support $\alpha$ Hya we have cast further afield, using high-precision observations made in support of our efforts by Carter (1994) in the South African Astronomical Observatory's *HKL* passbands, and measurements made in the ESO narrow band 10 $\mu$m filters (Bouchet *et al.* (1991), to whose published passbands (ESO User's Manual) we have added our calculated representative atmosphere for the La Silla site. To provide a traceable 5 $\mu$m magnitude for $\alpha$ Hya, we have used Koornneef's (1983) old ESO "M", with Bessell & Brett's (1988) recommended combination of this filter passband and atmosphere. In addition, we found the broad "N" magnitude by Thomas *et al.* (1973) to be useful. In order to use these photometric systems we required not only that cold filter profiles were available but also that zero points were traceable. This was facilitated by published observations of Sirius in all these passbands.

In this section we have fully described the pedigree of the photometry in Tables 4–8 and in Paper II, on which basis we adjusted the radiometric levels of spectral fragments from relative to absolute irradiances prior to the splicing procedures, and generated local "biases" (see below).

## 5. OUR ARCHIVE OF COMPOSITES

Tables 4–8 reproduce the header information that accompanies all five new composite spectra (cf. Paper II, Tables 2,

TABLE 4. "Header" information accompanying $\beta$ Peg composite.

3-10-92 OBSERVED SPECTRUM OF BETA PEGASI

$\beta$ Peg photometry file: photometry actually used to construct the spectrum

| Name | FWHM ($\mu$m) | Mag.±Unc. | Eff Wvl (Vega) ($\mu$m) | Eff Wvl (star) ($\mu$m) | $F_\lambda$ W cm$^{-2}$ $\mu$m$^{-1}$ |
|---|---|---|---|---|---|
| Kn | 0.0488 | -2.33±0.01 | 2.208 | 2.205 | 3.37E-13 |
| Ln | 0.1443 | -2.49±0.01 | 3.782 | 3.763 | 5.11E-14 |
| M | 0.6677 | -2.12±0.02 | 4.758 | 4.720 | 1.50E-14 |
| 8.7 | 1.1576 | -2.39±0.01 | 8.753 | 8.727 | 1.77E-15 |
| 11.7 | 1.2008 | -2.47±0.01 | 11.650 | 11.621 | 6.14E-16 |

Spectral fragments and portions of these actually used in observed spectrum (''used" may include combination with other data where overlaps occur)

| Fragment | Reference | Total range ($\mu$m) | Start and stop wavelengths ($\mu$m) | Average resolving power |
|---|---|---|---|---|
| NIR | 1 | 1.22-5.70 | 1.22-5.14 | 50 |
| KAO | 2 | 5.23-8.06 | 5.23-8.06 | 65,100 |
| 8-13 | 3 | 7.50-13.07 | 8.03-13.07 | 55,55,55 |
| LRS | 4 | 7.70-22.74 | 13.10-21.00 | 30 |
| LONG | 5 | 1.25-35.00 | 19.45-35.00 | - |

References:

- 1. Strecker, Erickson, and Witteborn 1979, Ap.J. Suppl., 41, 501.
- 2. FOGS data of August 5, 1986 KAO flight [$\beta$ Peg/$\alpha$ Lyr]; and Nov. 27-28 and 28-29, 1990 KAO flights [$\beta$ Peg/$\alpha$ Tau].
- 3. CGS3 UKIRT data of July 16, 1990 of M. Barlow (priv. comm. to MC) and Mt Lemmon FOGS data of Oct. 11 and 14, 1989 [$\beta$ Peg/$\alpha$ Lyr]; Barlow's CGS3 UKIRT data of Oct. 5, 1990 [$\beta$ Peg/$\alpha$ Tau]; and our previously defined $\alpha$ Tau 8--13 $\mu$m data.
- 4. LRS raw data extracted from ''LRSVAX" Groningen archive at NASA-Ames
- 5. Engelke Fn. used for T=3600K (see Blackwell, Lynas-Gray, and Petford 1991, A&A, 245, 567) and ang. diam. of 16.727 mas; we rescaled this to 16.98 mas. This Engelke Function was locked to the photometrically scaled combination of 8-13 and LRS spectra by splicing and used to replace the observations from 19.45 $\mu$m. A conservative error of 6.0% in EFn. due to effective temperature uncertainty was input for this fragment.

INFORMATION ON SPLICES AND BIASES INCURRED

| Process | Factor determined | ±Bias (%) |
|---|---|---|
| NIR cf. photometry | 1.025 | 0.90 |
| 813 cf. photometry | 1.029 | 0.64 |
| LRS blue/red bias | - | 0.16 |
| LRS splice to 813 | 0.995 | 0.01 |
| KAO joint splice to NIR and merged 813/LRS | 1.007 | 0.11 |
| Engelke Fn. splice to combined 813/LRS | 1.030 | 0.77 |

3, and 4 for the same pedigree for the $\alpha$ Tau composite). The date of original assembly appears, along with details of the photometry used to calibrate the composite radiometrically. The FWHM of the relevant passbands and their effective wavelengths for the Vega spectrum and for the star in question are recorded, along with the monochromatic specific intensities. All archival spectral fragments are detailed, with their total spectral ranges, the ranges of their data that were actually utilized, and their average resolving power over that spectral range (expressed as the resolving power, $\lambda/\Delta\lambda$). When several spectra are available, the relevant resolving powers are presented in the order in which the fragments are

TABLE 5. "Header" information accompanying $\alpha$ Boo composite.

4-28-93 OBSERVED SPECTRUM OF ALPHA BOOTIS

$\alpha$ Boo photometry file: photometry actually used to construct the spectrum

| Name | FWHM ($\mu$m) | Mag.±Unc. | Eff Wvl (Vega) ($\mu$m) | Eff Wvl (star) ($\mu$m) | $F_\lambda$ W cm$^{-2}$ $\mu$m$^{-1}$ |
|---|---|---|---|---|---|
| Kn | 0.0488 | -3.07±0.01 | 2.208 | 2.205 | 6.66E-13 |
| Ln | 0.1443 | -3.15±0.01 | 3.782 | 3.762 | 9.39E-14 |
| M | 0.6677 | -2.97±0.02 | 4.758 | 4.736 | 3.25E-14 |
| 8.7 | 1.1576 | -3.12±0.01 | 8.753 | 8.730 | 3.46E-15 |
| 11.7 | 1.2008 | -3.19±0.03 | 11.650 | 11.621 | 1.19E-15 |

Spectral fragments and portions of these actually used in observed spectrum (''used" may include combination with other data where overlaps occur)

| Fragment | Reference | Total range ($\mu$m) | Start and stop wavelengths ($\mu$m) | Average resolving power |
|---|---|---|---|---|
| NIR | 1 | 1.22-5.70 | 1.22-4.22 | 50 |
| KAO | 2 | 3.65-9.39 | 4.44-8.17 | 150 |
| 8-13 | 3 | 7.65-13.17 | 7.65-10.96 | 220,55 |
| LRS | 4 | 7.80-22.70 | 11.10-19.00 | 30 |
| LONG | 5 | 1.25-35.00 | 19.10-35.00 | - |

References:

- 1. Strecker, Erickson, and Witteborn 1979, Ap.J. Suppl., 41, 501.
- 2. FOGS data of May 11, 1992 KAO flight [$\alpha$ Boo/$\alpha$ Lyr].
- 3. FOGS Mt Lemmon data of Feb. 24, 1992 [$\alpha$ Boo/$\alpha$ Lyr] and CGS3 UKIRT data of May 24 and 25, 1991 (Barlow, priv. comm. to MC) [$\alpha$ Boo/$\beta$ Peg].
- 4. LRS raw data extracted from the new Groningen IRAS database and recalibrated with ''LRSCAL" routine in ''GIPSY" package.
- 5. Engelke Fn. used for T=4362K (see Blackwell, Lynas-Gray, and Petford 1991, A&A, 245, 567) and angular diameter=20.430 mas; we rescaled this to 20.80 mas. This Engelke Function was locked to the photometrically scaled combination of 8-13 and LRS spectra by splicing and used to replace the observations beyond 19.10 $\mu$m. A conservative error of 6.0% in EFn. due to effective temperature uncertainty was input for this fragment.

INFORMATION ON SPLICES AND BIASES INCURRED

| Process | Factor determined | ±Bias (%) |
|---|---|---|
| NIR cf. photometry | 1.002 | 0.89 |
| 813 cf. photometry | 1.056 | 0.85 |
| LRS blue/red bias | - | 0.03 |
| LRS splice to 813 | 0.933 | 0.03 |
| KAO joint splice to NIR and merged 813/LRS | 0.850 | 0.32 |
| Engelke Fn. splice to combined 813/LRS | 1.037 | 0.26 |

described in the "Reference" section accompanying each table. Although the actual spectral resolution is variable with wavelength in a composite spectrum, the degradation of higher resolution spectrum to match the resolutions of lower resolution spectra effectively leads to a low-resolution archive.

These six composites are rather similar at all wavelengths in their overall effective resolving powers, typically around 50. Of course, mere usage of a high-resolution grating does not of itself provide a high resolution product, because seeing conditions and spectrometer aperture all lead to a degradation in the resolution actually achieved. For example,

TABLE 6. "Header" information accompanying $\beta$ And composite.

10-15-93 OBSERVED SPECTRUM OF BETA ANDROMEDAE
$\beta$ And photometry file: photometry actually used to construct the spectrum

| Name | FWHM ($\mu$m) | Mag.±Unc. | Eff Wvl (Vega) ($\mu$m) | Eff Wvl (star) ($\mu$m) | $F_\lambda$ W cm$^{-2}$ $\mu$m$^{-1}$ |
|---|---|---|---|---|---|
| Kn | 0.0488 | -1.93±0.01 | 2.208 | 2.205 | 2.33E-13 |
| Ln | 0.1443 | -2.06±0.01 | 3.782 | 3.762 | 3.44E-14 |
| M | 0.6677 | -1.74±0.02 | 4.758 | 4.749 | 1.04E-14 |
| 8.7 | 1.1576 | -1.98±0.01 | 8.753 | 8.736 | 1.21E-15 |
| 11.7 | 1.2008 | -2.09±0.01 | 11.650 | 11.622 | 4.28E-16 |

Spectral fragments and portions of these actually used in observed spectrum
(''used" may include combination with other data where overlaps occur)

| Fragment | Reference | Total range ($\mu$m) | Start and stop wavelengths ($\mu$m) | Average resolving power |
|---|---|---|---|---|
| NIR | 1 | 1.22-5.50 | 1.22-4.14 | 50 |
| KAO | 2 | 3.38-10.12 | 4.26-7.89 | 50,50,45,70,150 |
| 8-13 | 3 | 7.59-13.06 | 7.59-13.06 | 65,55 |
| LRS | 4 | 7.70-22.60 | 7.70-16.90 | 30 |
| LONG | 5 | 15.52-24.09 | 16.95-23.37 | 73 |
| VERY-LONG | 6 | 1.25-35.00 | 12.00-35.00 | - |

References:

- 1. Strecker, Erickson, and Witteborn 1979, Ap.J. Suppl., 41, 501.
- 2. FOGS data of Nov. 29, 1983, Dec. 1, 1983, and Dec. 12, 1985 KAO flights [$\beta$ And/$\alpha$ Tau]; Jan. 18, 1991 FOGS and SIRAS data [$\beta$ And/$\alpha$ CMa]; and HIFOGS KAO flight of July 21, 1993 [$\beta$ And/$\alpha$ Lyr].
- 3. FOGS Mt Lemmon data of Sept. 17, 1985 [$\beta$ And/$\beta$ Peg] and UKIRT CGS3 data of August 29, 1993 [$\beta$ And/$\alpha$ CMa] and [$\beta$ And/$\alpha$ Tau].
- 4. LRS raw data extracted from the new Groningen IRAS database and recalibrated with ''LRSCAL" routine in ''GIPSY" package.
- 5. UKIRT CGS3 20 um ratio of [$\beta$ And/$\alpha$ Tau] of Oct. 5, 1990.
- 6. Engelke Fn. used for T=3839K (see Blackwell, Lynas-Gray, and Petford 1991, A&A, 245, 567) and angular diameter=13.219 milliarcsec; we rescaled this to 13.71 mas. This Engelke Function was locked to the photometrically scaled combination of 8-13, LRS, and LONG spectra by splicing and used to replace the observations beyond 12.00 $\mu$m (bias only ±0.16%). The uncertainty in EFn. due to an effective temperature error of 100K is 2.7% which was input as the error of this fragment because of the additional shape constraints available from the LONG spectral fragment.

INFORMATION ON SPLICES AND BIASES INCURRED

| Process | Factor determined | ±Bias (%) |
|---|---|---|
| NIR cf. photometry | 0.983 | 0.90 |
| 813 cf. photometry | 0.997 | 0.66 |
| LRS blue/red bias | - | 0.07 |
| LRS splice to 813 | 0.941 | 0.14 |
| KAO joint splice to NIR and merged 813/LRS | 0.881 | 0.05 |
| Engelke Fn. splice to combined 813/LRS/CGS3-20$\mu$m | 1.075 | 0.16 |

SEWs circular variable filter wheel was a 1.5% device, capable of a formal resolving power of 70. But its use on the KAO with apertures of 30–40″ surely lowered this power to around 50.

Note that the maximum possible wavelength coverage was used to constrain any splice and to enhance signal-to-noise ratios in regions of overlapping independent data. Subsequently, we select a specific wavelength above which we use one fragment, and below, the other. However, the lower spectral resolution fragment at this juncture may embody

TABLE 7. "Header" information accompanying $\beta$ Gem composite.

**09-12-94 OBSERVED SPECTRUM OF BETA GEMINORUM**

**$\beta$ Gem photometry file: photometry actually used to construct the spectrum**

| Name | FWHM ($\mu$m) | Mag.±Unc. | Eff Wvl (Vega) ($\mu$m) | Eff Wvl (star) ($\mu$m) | $F_\lambda$ W cm$^{-2}$ $\mu$m$^{-1}$ |
|---|---|---|---|---|---|
| Kn | 0.0488 | -1.14±0.02 | 2.208 | 2.205 | 1.13E-13 |
| Ln | 0.1443 | -1.21±0.02 | 3.782 | 3.762 | 1.57E-14 |
| M | 0.6677 | -1.13±0.02 | 4.758 | 4.733 | 5.95E-15 |
| 8.7 | 1.1576 | -1.21±0.02 | 8.753 | 8.725 | 5.96E-16 |
| 11.7 | 1.2008 | -1.22±0.02 | 11.650 | 11.623 | 1.94E-16 |

**Spectral fragments and portions of these actually used in observed spectrum ("used" may include combination with other data where overlaps occur)**

| Fragment | Reference | Total range ($\mu$m) | Start and stop wavelengths ($\mu$m) | Average resolving power |
|---|---|---|---|---|
| NIR | 1 | 1.22-5.66 | 1.22-4.90 | 50 |
| KAO | 2 | 4.92-9.39 | 4.92-7.63 | 150 |
| 8-13 | 3 | 7.67-12.83 | 7.67-10.38 | 55 |
| LRS | 4 | 7.80-22.60 | 10.39-12.94 | 30 |
| LONG | 5 | 16.14-24.61 | 16.26-24.02 | 73 |
| VERY-LONG | 6 | 1.25-35.00 | 12.95-35.00 | - |

**References:**

- **1. Strecker, Erickson, and Witteborn 1979, Ap.J. Suppl., 41, 501.**
- **2. HIFOGS data of Dec. 21, 1991 KAO flight [$\beta$ Gem/$\alpha$ CMa].**
- **3. CGS3 UKIRT data of Nov. 5, 1993 [$\beta$ Gem/$\alpha$ Tau] (multiplied by CGS3 UKIRT [$\alpha$ Tau/$\alpha$ CMa] from Nov. 9, 1991). Confirmed by UKIRT CGS3 [$\beta$ Gem/$\alpha$ CMa] of Nov. 3 and 4, 1993.**
- **4. LRS raw data extracted from the new Groningen IRAS database and recalibrated with "LRSCAL" routine in "GIPSY" package.**
- **5. CGS3 UKIRT 20 $\mu$m ratio of [$\beta$ Gem/$\alpha$ CMa] of Feb. 7, 1994 from the UKIRT archives.**
- **6. Engelke Fn. used for T=4866K (see Blackwell, Lynas-Gray, and Petford 1991, A&A, 245, 567) and ang. diam.=7.807 milliarcsec; we rescaled this to 8.07 mas. This Engelke Function was locked to the photometrically scaled combination of 8-13, LRS, and LONG spectra by splicing and used to replace the observations beyond 12.95 $\mu$m (bias ±0.14%). The uncertainty in EFn. due to an effective temperature error of 100K is 2.1% which was input as the uncertainty in this extrapolating fragment because of the additional shape constraints available from the LONG spectral fragment.**

**INFORMATION ON SPLICES AND BIASES INCURRED**

| Process | Factor determined | ±Bias (%) |
|---|---|---|
| NIR cf. photometry | 1.020 | 1.26 |
| 813 cf. photometry | 1.019 | 1.03 |
| LRS blue/red bias | - | 0.09 |
| LRS splice to 813 | 1.115 | 0.33 |
| KAO joint splice to NIR and merged 813/LRS | 1.025 | 0.06 |
| Engelke Fn. splice to combined 813/LRS/CGS3-20$\mu$m | 1.052 | 0.14 |

inverse-variance weighted combined data from both spectra in the overlap region, changing the original fragment (as described above in Sec. 2), so these wavelength cutoffs are not rigid. Information also appears on all processes undertaken during assembly, with their results (scale factor and uncertainties or "biases"). Scale factors best match spectral fragments to the observed in-band fluxes from photometry, while biases represent the uncertainties associated with each scale

TABLE 8. "Header" information accompanying $\alpha$ Hya composite.

12-12-94 OBSERVED SPECTRUM OF ALPHA HYDRAE

$\alpha$ Hya photometry file: photometry actually used to construct the spectrum

| Name | FWHM ($\mu$m) | Mag.±Unc. | Eff Wvl (Vega) ($\mu$m) | Eff Wvl (star) ($\mu$m) | $F_\lambda$ W cm$^{-2}$ $\mu$m$^{-1}$ | Source |
|---|---|---|---|---|---|---|
| SAAO-H | 0.2896 | -1.074±0.015 | 1.655 | 1.638 | 3.09E-13 | Carter 1994 |
| SAAO-K | 0.3902 | -1.223±0.016 | 2.221 | 2.219 | 1.19E-13 | Carter 1994 |
| SAAO-L | 0.5648 | -1.341±0.010 | 3.474 | 3.459 | 2.46E-14 | Carter 1994 |
| M | 0.5418 | -1.107±0.042 | 4.748 | 4.764 | 5.87E-15 | Koornneef 1983 |
| ESO-M | 0.3588 | -1.166±0.042 | 4.733 | 4.714 | 6.28E-15 | Bouchet et al. 1989 |
| ESO-N1 | 0.8954 | -1.280±0.051 | 8.373 | 8.369 | 7.50E-16 | Bouchet et al. 1989 |
| ESO-N2 | 1.2949 | -1.324±0.039 | 9.849 | 9.860 | 3.74E-16 | Bouchet et al. 1989 |
| ESO-N3 | 1.2381 | -1.424±0.054 | 12.567 | 12.538 | 1.72E-16 | Bouchet et al. 1989 |
| N | 5.1318 | -1.32 ±0.036 | 10.161 | 10.219 | 3.25E-16 | Thomas et al. 1973 |

Spectral fragments and portions of these actually used in observed spectrum (''used" may include combination with other data where overlaps occur)

| Fragment | Reference | Total range ($\mu$m) | Start and stop wavelengths ($\mu$m) | Average resolving power |
|---|---|---|---|---|
| NIR | 1 | 1.24-5.46 | 1.24-5.46 | 50 |
| KAO | 2 | 5.20-8.00 | 5.20-8.00 | 150 |
| 8-13 | 3 | 7.59-13.31 | 7.59-13.31 | 55 |
| LRS | 4 | 7.67-22.74 | 8.05-22.74 | 30 |
| LONG | 5 | 1.25-35.00 | 10.65-35.00 | – |

References:

- 1. Strecker, Erickson, and Witteborn 1979, Ap.J. Suppl., 41, 501; actually used fragment for $\gamma^1$ And, K3-IIb.
- 2. FOGS data of April 17, 1990 KAO flight [$\alpha$ Hya/$\alpha$ CMa] in New Zealand.
- 3. CGS3 UKIRT data of Feb. 9, 1993 [$\alpha$ Hya/$\alpha$ CMa].
- 4. LRSVAX version of Groningen database at NASA-Ames; spliced and recalibrated.
- 5. Engelke Fn. used for T=4141K (see Bell 1993, MNRAS, 264, 345); we found the best fitting ang. diam. to be 9.27 milliarcsec. This Engelke Function was locked to the photometrically scaled combination of 8-13 and the LRS, by ''splicing" and used to replace the observations beyond 10.65 $\mu$m with a conservative estimated uncertainty in EFn. of 6%.

INFORMATION ON SPLICES AND BIASES INCURRED

| Process | Factor determined | ±Bias (%) |
|---|---|---|
| NIR cf. photometry | 1.473 | 0.50 |
| 813 cf. photometry | 0.777 | 2.61 |
| LRS blue/red bias | – | 0.23 |
| LRS splice to 813 | 0.888 | 0.40 |
| KAO joint splice to NIR and merged 813/LRS | 0.993 | 0.63 |
| Engelke Fn. splice to combined 813/LRS/CGS3-20$\mu$m | 0.860 | 0.37 |

factor. Biases, therefore, are correlated errors that represent entire ranges of the overall spectrum, rather than the uncorrelated errors that are specific to each individual wavelength point. Two kinds of bias occur: "local" biases arising from scaling of spectral fragments; and "global" that derive directly from the underpinning uncertainty in the absolute calibrations of Vega and Sirius (Paper I).

We prefer to provide pristine data whenever possible, rather than to regrid each composite to some equally spaced or common wavelength scale. Each composite, therefore, has a different set of wavelengths. We tabulate wavelength; monochromatic specific intensity ($F_\lambda$ in units of W cm$^{-2}$ $\mu$m$^{-1}$); total uncertainty (also in units of W cm$^{-2}$ $\mu$m$^{-1}$) associated with this value of $F_\lambda$; local bias;

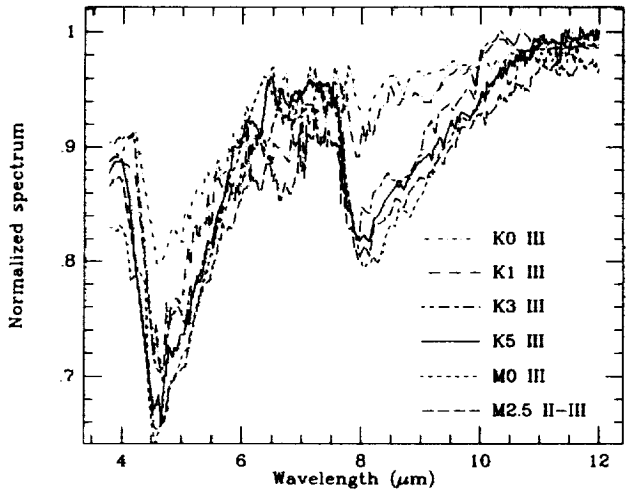


FIG. 7. The six observed composite spectra in the regions of the CO and SiO fundamentals, plotted in $\lambda^4 F_\lambda$ space, each normalized by their mean level between 12 and 35 $\mu$m. Each star has a different line type and one can see a progression of deeper bands with cooler stars.

and global bias. For most applications, "total uncertainty" is the error term most appropriate to use. It is the standard deviation of the spectral irradiance and includes the local and global biases. Local and global biases are given as a percent of the irradiance. The global bias does not contribute error to flux ratios or color measurements, and may be removed (in the root-sum-square sense) from the total error.

Figure 7 offers a direct comparison of these six composite spectra in the region containing the dominant spectral structure due to the fundamentals of CO and SiO. To intercompare different stars one would ideally normalize all spectra using a subregion of the wavelength region of interest. One might think that the 6.5–7.5 $\mu$m region between CO and SiO would be the natural region in which to normalize. However, the onset of water vapor absorption near 6.5 $\mu$m makes this region unsuitable (the absorption is clearest for the coolest star, $\beta$ Peg, but is also shown by $\beta$ And). Consequently, we have adjusted them according to their average levels between 12 and 35 $\mu$m, where there is no significant observed structure. To mitigate the very steep decay of flux densities in these stellar spectra we have again treated all spectra in $\lambda^4 F_\lambda$ space. There are some slight differences in overall curvature between stars in Fig. 7, solely due to their different temperatures, but one can clearly see that there is an essentially monotonic progression in absorption band depths with lateness of spectral type (although $\beta$ Peg does not always have the lowest spectrum—perhaps its higher luminosity class invalidates this direct comparison with the other class III giants).

## 6. CONCLUSIONS

We have assembled absolutely calibrated, complete, continuous stellar spectra for six stars: $\alpha$ Tau, $\beta$ Peg, $\alpha$ Boo, $\beta$ And, $\beta$ Gem, and $\alpha$ Hya. These spectra are tightly constrained by carefully characterized photometry and have an estimated absolute uncertainty of order 3% ($1\sigma$) across most of the 1.2–35 $\mu$m range. Such spectra establish the pedigree for secondary stellar standards and thereby the flexibility to calibrate arbitrary filter systems and sensors on the ground, from airplanes, or satellites. These composite spectra with their associated pedigree files can be obtained through NASA's ADC at the Goddard Space Flight Center.

We thank Phillips Laboratory for its support of this effort through Dr. S. D. Price under Contract No. F19628-92-C-0900 with JS&E, Inc. (MC, RGW). We are grateful to NASA's Airborne Astronomy program for its continued support and to the staff of the entire KAO program for their sterling efforts throughout the flights dedicated to this calibration study. MC also thanks the NASA–Ames Research Center for partial support under Co-Operative Agreement No. NCC 2-142 with Berkeley. We are grateful to Dr. W. Glaccum for providing access to his uniquely valuable KAO archive of stellar spectra.

## APPENDIX

### *1. Data Available on the AAS CD-ROM Series*

The digital (ASCII) version of the six calibrated stellar spectra portrayed in Fig. 4 can be found in the Fifth volume of the AAS CD-ROM series. These are represented as five-column files, with the detailed structure given in Sec. 5, paragraph 4. In addition, we have archived the two calibrated Kurucz model spectra for Vega and Sirius on the CD-ROM. These appear as five-column files with the same structure as the six stellar spectra.

## REFERENCES

Aumann, G., *et al.* 1984, ApJ, 278, L23
Bell, R. 1993, MNRAS, 264, 345
Bessell, M. S. & Brett, J. M. 1988, PASP, 100, 1134
Blackwell, D. E., & Lynas-Gray, A. E. 1994, A&A, 282, 899
Blackwell, D. E., Lynas-Gray, A. E., & Petford, A. D. 1991, A&A, 245, 567
Bouchet, P., Moneti, A., Slezak, E., Le Bertre, T., & Manfroid, J. 1991, A&AS, 80, 379
Carbon, D. F. 1994 (private communication)
Carter, B. 1994 (private communication)
Cohen, M., & Barlow, M. J. 1974, ApJ, 193, 401
Cohen, M., & Barlow, M. J. 1980, ApJ, 238, 585
Cohen, M., & Davies, J. K. 1995, MNRAS (in press) (Paper V)
Cohen, M., Walker, R. G., Barlow, M. J., & Deacon, J. R. 1992a, AJ, 104, 1650 (Paper I)
Cohen, M., Witteborn, F. C., Carbon, D. F., Augason, G. C., Wooden, D., Bregman, J., & Goorvitch, D. 1992b, AJ, 104, 2045 (Paper III)
Cohen, M., Walker, R. G., & Witteborn, F. C. 1992, AJ, 104, 2030 (Paper II)
Deacon, J. R. 1991, Ph.D. dissertation, University College London
Engelke, C. W. 1992, AJ, 104, 1248
Gehrz, R. D., Hackwell, J. A., and Jones, T. W. 1974, ApJ, 191, 675
Glaccum, W. 1990, Ph.D. dissertation, University of Chicago
Hammersley, P. L. 1994 (private communication of October 26, 1994)
Hanner, M. S. 1994 (private communication of May 25, 1994)
*IRAS* Point Source Catalog, version 2, 1988, IRAS Catalogs and Atlases, Volumes 2–6, NASA RP-1190 (GPO, Washington, DC)

Kleinmann, S. G., Cutri, R. M., Young, E. T., Low, F. J., & Gillett, F. C. 1986, Explanatory Supplement to the IRAS Serendipitous Catalog (GPO, Washington, DC)
Koornneff, J. 1983, A&AS, 51, 489
Leggett, S. K. 1994 (private communication of June 18, 1994)
Leggett, S. K., Mountain, C. M. Selby, M. J., Blackwell, D. E., Booth, A. J., Haddock, D. J., & Petford, A. D. 1986, A&A, 159, 217
Lord, S. D. 1992, A New Software Tool for Computing the Earth's Atmospheric Transmission of Near-Infrared and Far-Infrared Radiation, NASA TM-103957
McGregor, A. D. 1977, Imperial College of Science & Technology UK Detector Testing Contract: Final Report, Royal Observatory of Edinburgh
Moseley, S. H., Dwek, E., Glaccum, W., Graham, J. R., Loewenstein, R. F., & Silverberg, R. F. 1989, ApJ, 347, 1119
Mountain, C. M. 1994 (private communication of June 24, 1994)
Mountain, C. M., Leggett, S. K., Selby, M. J., Blackwell, D. E. & Petford, A. D. 1985, A&A, 151, 399
Petford, A. D. 1994 (private communication of June 20, 1994)
Selby M. J., *et al.* 1988, A&AS, 74, 127
Strecker, D. W., Erickson, E. F., & Witteborn, F. C. 1979, ApJS, 41, 501
Thomas, J. A., Hyland, A. R., & Robinson, G. 1973, MNRAS, 165, 201
Witteborn, F. C., & Bregman, J. D. 1984, Proc. Soc. Photo-Opt. Instrum. Eng., 509, 123
Witteborn, F. C., Cohen, M., Bregman, J. D., Heere, K. R., Greene, T. P., & Wooden, D. H. 1995, in Proceedings of the Airborne Astronomy Symposium on the Galactic Ecosystem, edited by M. Haas, E. F. Erickson, and J. Davidson, ASP Conf. Ser. Vol. 73, p. 573
Wooden, D. H. 1989, in Proceedings of the ESO/SIPC Workshop, SN 1987A and Other Supernovae, edited by I. J. Danziger and K. Kjar (ESO, Garching), p. 531
Wooden, D. H., *et al.* 1993, ApJS, 88, 477
Young, E. T., Neugebauer, G., Kopan, E. L., Benson, R. D., Conrow, T. P., Rice, W. L., & Gregorich, D. T. 1985, A User's Guide to IRAS Pointed Observation Products (Ipac, Pasadena)